Journal of the Egyptian Mathematical Society 25 (2017) 230–237

Contents lists available at ScienceDirect

Journal of the Egyptian Mathematical Society

journal homepage: www.elsevier.com/locate/joems

Original Article

# Impact of anisotropic slip on transient three dimensional MHD flow of ferrofluid over an inclined radiate stretching surface

A.M. Rashad

*Department of Mathematics, Aswan University, Faculty of Science, Aswan, 81528, Egypt*

ARTICLE INFO

*Article history:*
Received 6 June 2016
Revised 28 August 2016
Accepted 19 December 2016
Available online 26 January 2017

*MSC:*
MHD
76W99
76D10

*Keyword:*
Ferrofluid
Thermal radiation
Anisotropic slip
Transient flow

ABSTRACT

The present study explores the impact of anistropic slip on transient three dimensional MHD flow of Cobalt-kerosene ferrofluid over an inclined radiate stretching surface. The governing partial differential equations for this study are solved by the Thomas algorithm with finite-difference type. The impacts of several significant parameters on flow and heat transfer characteristics are exhibited graphically. The conclusion is revealed that the local Nusselt number is significantly promoted due to influence of thermal radiation whereas diminished with elevating the solid volume fraction, magnet parameter and slip factors. Further, the skin friction coefficients visualizes a considerable enhancement with boosting the magnet and radiation parameters, but a prominent reduction is recorded by elevating the solid volume fraction and slip factors.



## 1. Introduction

Magnetohydrodynamics (MHD) of fluid flows plays a crucial role in the field of medicine, which is accounted in cancer tumour treatment causing hypothermia, reducing bleeding in case of severe injuries, magnetic resonance imaging and several other diagnostic tests [1,2]. Likewise, the electromagnetic forces not only influence the mechanics of the system but also affect the thermodynamics of the system through thermal radiation. In fact, the consideration of thermal radiation when analyzing the heat transfer characteristics plays a pivotal function in processes involving rise temperature. The efficiency of many biomedical engineering, gas-cooled nuclear reactors, food industries and mode of energy transfer in hypersonic flights. Some researchers have reported that the thermal radiation is an effective homogeneous heating method when it is studied along with magnetic field [3–5].

The analysis of Nanofluids flow has been subject of comprehensive explore resultant in rising thermal conductivity heat transfer procedure. Nanofluid is envisaged to refer a fluid in which nanometer-magnitude particles are suspended in classical heat transfer essential fluids [6,7]. Classical heat transfer fluids, encompassing oil, water, and ethylene glycol blend are pauper heat transfer fluids. Nanofluids are utilized in numerous engineering applications like microelectronics, micro fluidics, heat interchangers and refrigerating of electronic apparatuses. A reliable studies to this fascinating topic along with the theoretical patterns or experimental data is well authenticated in the literature [8–16]. To be more particular the magnetic nanofluids (Ferrofluids) which are colloidal suspensions of magnetic nanoparticles like cobalt, magnetite and ferrite scattered in a non-conducting liquids such as kerosene, water, heptane and hydro-carbons. Ferrofluids are pretty helpful in diverse engineering applications such as for example in intelligent biomaterials for wound treatment, medicine drug targeting, megaphones, and bumpers and revolving exception seals. A comprehensive monographs of the studies of to ferrofluids along with their different applications is found in the following literatures in [17–20]. Recently, Malvandi et al. [21] studied the influence of nanoparticle migration on thermal performance of ferrofluid flow inside a vertical micro-annulus. Heysiattalab et al. [22] investigated the anisotropic manner of ferrofluids at filmwise intensification over a vertical plate with a variable directional magnetic field. Malvandi et al. [23] have also considered a theoretical study of condensate falling film of ferrofluids in the presence of anisotropic behavior of thermal conductivity and nanoparticle migration effects. Rashad [24] studied the effect of partial slip on MHD mixed convection flow of ferrofluid over a non-isothermal radiate wedge.

The intent of the current investigation is to examine the impact of anisotropic slip on the transient MHD three-dimensional laminar flow of ferrofluid along a radiate stretching surface. The

*E-mail address:* am_rashad@yahoo.com

http://dx.doi.org/10.1016/j.joems.2016.12.001

**Nomenclature**

| | |
|---|---|
| $b$ | *constant* ($s^{-1}$) |
| $B_0$ | magnitude of magnetic field (T) |
| $C_{fx}$, $C_{fy}$ | local skin friction coefficients in the x- and y-orientations |
| $C_p$ | specific heat (J $kg^{-1}$ $K^{-1}$) |
| $f'$ | x-velocity component |
| $g$ | x-velocity component |
| $g^*$ | gravitational acceleration (m $s^{-2}$) |
| $G$ | dimensionless pressure |
| $Gr_x$ | local Grashof number |
| $h$ | velocity in y-tendency |
| $H$ | surface temperature excess ratio |
| $Ha$ | magnet parameter |
| $k$ | thermal conductivity (W $m^{-1}$ $K^{-1}$) |
| $N_1$, $N_2$ | slip coefficients in the x- and y- orientations ($m^2$ s $kg^{-1}$) |
| $Nu_x$ | local Nusselt number |
| $P$ | pressure (N $m^{-2}$) |
| $Pr$ | Prandtl number |
| $q_r$ | radiative heat transfer (W $m^{-2}$) |
| $q_w$ | wall heat flux (W $m^{-2}$) |
| $Rd$ | thermal radiation parameter |
| $Re_x$ | local Reynolds number |
| $t$ | dimensional time (s) |
| $T$ | ferrofluid temperature (K) |
| $u$, $v$, $w$ | velocity components in the x, y, and z-orientations (m $s^{-1}$) |
| $x$, $y$, $z$ | Cartesian coordinates (m) |

*Greek symbols*

| | |
|---|---|
| $\alpha$ | thermal diffusivity ($m^2$ $s^{-1}$) |
| $\beta$ | thermal expansion coefficient ($K^{-1}$) |
| $\beta_R$ | absorption coefficient ($m^{-1}$) |
| $\eta$ | similarity variable |
| $\theta$ | dimensionless ferrofluid temperature |
| $\delta_1$, $\delta_2$ | slip factors |
| $\mu$ | dynamic viscosity (kg $m^{-1}s^{-1}$) |
| $\upsilon$ | kinematic viscosity of base fluid ($m^2$ $s^{-1}$) |
| $\Omega$ | inclination angle |
| $\rho$ | density (Kg $m^{-3}$) |
| $\sigma_1$ | Stefan-Boltzmann constant ($m^2$ kg $s^{-2}$ $K^1$) |
| $\sigma$ | electrical conductivity (s $m^{-1}$) |
| $\phi$ | solid volume fraction |
| $\tau$ | dimensionless time |

*Subscripts*

| | |
|---|---|
| $f$ | base fluid (kerosene) |
| $ff$ | ferrofluid |
| $s$ | ferromagnetic particle (cobalt) |
| $w$ | condition at the wall |
| $\infty$ | condition at infinity |

governing equations are solved computationally and the flow and convective heat transfer are discussed with corresponding figures.

## 2. Mathematical formulation

Consider a three-dimensional, laminar, transient MHD flow of ferrofluid over a semi-infinite inclined plate moving in the *x*-orientation with a velocity *bx* and subject to anisotropic slip and thermal radiation impacts. The *y*-orientation is inclined at an angularity Ω to the horizontal streak, whilst the *z*-orientation is perpendicular to the plate surface, see Fig. 1. The surface has a

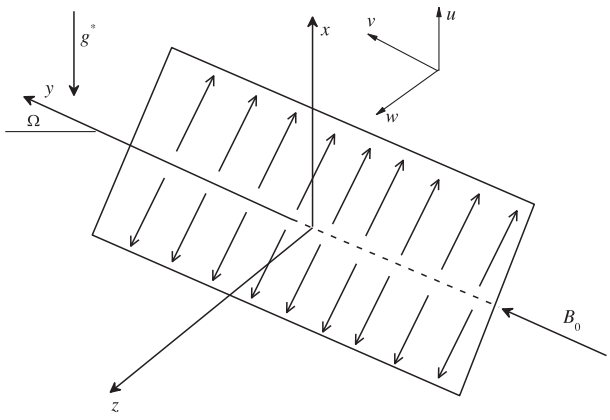


**Fig. 1.** Physical model and coordinate system.

**Table 1**
Thermophysical properties of kerosene and cobalt solids [25].

| Property | Kerosene | Cobalt |
|---|---|---|
| $\rho$ (kg $m^{-3}$) | 780 | 8900 |
| $C_p$ (J$kg^{-1}$ $K^{-1}$) | 2090 | 420 |
| k (W $m^{-1}$ $K^{-1}$) | 0.149 | 100 |
| $\beta$ ($K^{-1}$) | $9.9 \times 10^{-4}$ | $1.3 \times 10^{-5}$ |
| $\sigma$ (Simens/m) | $6 \times 10^{-10}$ | $1.602 \times 10^{7}$ |
| μ (kg$^{-1}$ $m^{-1}$ $s^{-1}$) | 0.00164 | – |

uniform temperature $T_w$ and the uniform temperature of ambient fluid is $T_\infty$. The magnitude of magnetic field $B_0$ is utilized in the y- orientation. This stimulates the magnetic effectiveness in the *x*- and z-orientations.

Thermophysical properties of the ferrofluid are presented in Table 1.

The basic governing equations for ferrofluid using the above assumptions with Boussinesq and boundary-layer approximations are [26]:

$$\frac{\partial u}{\partial x} + \frac{\partial w}{\partial z} = 0, \tag{1}$$

$$\frac{\partial u}{\partial t} + u\frac{\partial u}{\partial x} + w\frac{\partial u}{\partial z} = \frac{1}{\rho_{ff}} \times \left[\mu_{ff}\frac{\partial^2 u}{\partial z^2} + g^*(\rho\beta)_{ff}\cos\Omega(T - T_\infty) - \sigma_{ff}B_0^2 u\right], \tag{2}$$

$$\frac{\partial v}{\partial t} + w\frac{\partial v}{\partial z} = \frac{1}{\rho_{ff}}\left[\mu_{ff}\frac{\partial^2 v}{\partial z^2} + g^*(\rho\beta)_{ff}\sin\Omega(T - T_\infty)\right], \tag{3}$$

$$\frac{\partial w}{\partial t} + w\frac{\partial w}{\partial z} = \frac{1}{\rho_{ff}}\left[-\frac{\partial p}{\partial z} + \mu_{ff}\frac{\partial^2 w}{\partial z^2} - \sigma_{ff}B_0^2 w\right], \tag{4}$$

$$\frac{\partial T}{\partial t} + w\frac{\partial T}{\partial z} = \alpha_{ff}\frac{\partial^2 T}{\partial z^2} - \frac{1}{(\rho C_p)_{ff}}\frac{\partial q_r}{\partial z}, \tag{5}$$

The appropriate boundary conditions of the investigation are:

$$u(t,x,0) = bx + N_1\mu_{ff}\frac{\partial u}{\partial z}, \quad v(t,x,0) = N_2\mu_{ff}\frac{\partial v}{\partial z}, \quad w(t,x,0) = 0, \quad T(t,x,0) = T_w, \quad u(t,x,\infty) = 0, \quad v(t,x,\infty) = 0, \quad T(t,x,\infty) = T_\infty, \quad \frac{\partial w}{\partial z}(t,x,\infty) = 0 \tag{6}$$

where *x*, *y*, and *z* are the Cartesian coordinates. *u*, *v*, *w*, *P* and *T* are the velocity components in the *x*, *y*, and *z*-orientations, pressure and ferrofluid temperature, respectively. $g^*$, *b*, *t*, and Ω are the gravitational acceleration, constant, dimensional time and the inclination angle, respectively. $N_1$ and $N_2$ are the slip coefficients

in the $x$- and y- orientations, respectively. $\beta_{ff}$ is the thermal expansion coefficient of the ferrofluid; $\rho_{ff}$ is the ferrofluid density, $\mu_{ff}$ is the dynamic viscosity of the ferrofluid and $\alpha_{ff}$ is the thermal diffusivity of the ferrofluid, $(\rho C_p)_{ff}$ is the heat capacitance of ferrofluid, $\sigma_{ff}$ is the electrical conductivity the ferrofluid which are given by [8,27];

$$\rho_{ff} = (1-\phi)\rho_f + \phi\rho_s, \quad \mu_{ff} = \frac{\mu_f}{(1-\phi)^{2.5}},$$

$$\alpha_{ff} = \frac{k_{ff}}{(\rho C_p)_{ff}}, \quad (\rho C_p)_{ff} = (1-\phi)(\rho C_p)_f + \phi(\rho C_p)_s,$$

$$(\rho\beta)_{ff} = (1-\phi)(\rho\beta)_f + \phi(\rho\beta)_s, \quad \frac{k_{ff}}{k_f} = \frac{(k_s+2k_f)-2\phi(k_f-k_s)}{(k_s+2k_f)+\phi(k_f-k_s)},$$

$$\frac{\sigma_{ff}}{\sigma_f} = 1 + \frac{3(\sigma_s/\sigma_f - 1)\phi}{(\sigma_s/\sigma_f + 2) - (\sigma_s/\sigma_f - 1)\phi} \tag{7}$$

Here subscripts "*ff*", "*f*" and "*s*" stand for the properties of the ferrofluid, base fluid (kerosene) and ferromagnetic particle (cobalt) respectively. $\phi$ is the solid volume fraction, $k_{ff}$ is the thermal conductivity of ferrofluid.

The radiative heat transfer in z-orientation is simplified by the Rosseland approximation is defined as [28];

$$q_r = -\frac{4\sigma_1}{3\beta_R}\frac{\partial T^4}{\partial z} = -\frac{16\sigma_1 T^3}{3\beta_R}\frac{\partial T}{\partial z}, \tag{8}$$

with $\sigma_1$ is the Stefan–Boltzmann constant, $\beta_R$ is the absorption coefficient.

Introducing the following non-dimensional quantities

$$\tau = bt, \quad \eta = z/\sqrt{\upsilon_f t}, \quad u = bxf'(\tau,\eta) + \Gamma\cos\Omega g(\tau,\eta),$$

$$v = \Gamma\sin\Omega h(\tau,\eta), \quad w = -\sqrt{b^2\upsilon_f t}\, f, \quad \Gamma = \frac{g^*\beta_f(T_f - T_\infty)}{b},$$

$$\theta(\tau,\eta) = (T-T_\infty)/(T_w - T_\infty), \quad P = \rho_f b\upsilon_f G(\tau,\eta),$$

$$Ha = B_0\sqrt{\sigma_f/\rho_f b}, \quad \delta_1 = N_1\mu_f\sqrt{b/\upsilon_f}, \quad \delta_2 = N_2\mu_f\sqrt{b/\upsilon_f},$$

$$\delta = \delta_2/\delta_1, \quad Rd = 4\sigma T_\infty^3/\beta_R k_f, \quad H = T_f/T_\infty, \quad \Pr = \upsilon_f/\alpha_f \tag{9}$$

In view of the Eq. (9), the basic field of Eqs. (1)–(6) with Eqs. (7) and (8) can be expressed in non-dimensional form as;

$$\Gamma_1 f''' + \frac{\eta}{2}f'' + \tau\left(ff'' - f'^2 - \Gamma_2 Ha^2\left(\sigma_{ff}/\sigma_f\right)f'\right) - \tau\frac{\partial f'}{\partial\tau} = 0, \tag{10}$$

$$\Gamma_1 g'' + \frac{\eta}{2}g' + \tau\left(fg' - f'g - \Gamma_2 Ha^2\left(\sigma_{ff}/\sigma_f\right)g + \Gamma_2\theta\right) - \tau\frac{\partial g}{\partial\tau} = 0, \tag{11}$$

$$\Gamma_1 h'' + \frac{\eta}{2}h' + \tau\left(fh' + \Gamma_3\theta\right) - \tau\frac{\partial h}{\partial\tau} = 0, \tag{12}$$

$$\Gamma_2 G' + \Gamma_1 f'' + \frac{\eta}{2}f' - \frac{1}{2}f + \tau\left(ff' - \Gamma_2 Ha^2(\sigma_{ff}/\sigma_f)f\right) - \tau\frac{\partial f}{\partial\tau} = 0, \tag{13}$$

$$\frac{\Gamma_4}{\Pr}\left(\frac{k_{ff}}{k_f}\right)\theta'' + \frac{\Gamma_4}{\Pr}\frac{4Rd}{3}\left\{\theta'[(H-1)\theta+1]^3\right\}' + \frac{\eta}{2}\theta' + \tau f\theta' - \tau\frac{\partial\theta}{\partial\tau} = 0, \tag{14}$$

$$f(\tau,0) = 0, \quad f'(\tau,0) = 1 + \frac{\delta_1}{(1-\phi)^{2.5}}\tau^{-1/2}f''(\tau,0),$$

$$g(\tau,0) = \frac{\delta_1}{(1-\phi)^{2.5}}\tau^{-1/2}g'(\tau,0), \quad G(\tau,0) = 0,$$

$$h(\tau,0) = \frac{\delta_2}{(1-\phi)^{2.5}}\tau^{-1/2}h'(\tau,0), \quad \theta(\tau,0) = 1,$$

$$f'(\tau,\infty) = g(\tau,\infty) = h(\tau,\infty) = \theta(\tau,\infty) = 0 \tag{15}$$

In Eqs. (10)–(15), a prime denotes partial differentiation with respect to $\eta$, and the parameters $\Gamma_1$, $\Gamma_2$, $\Gamma_3$ and $\Gamma_4$ are given by;

$$\Gamma_1(\phi) = \frac{1}{(1-\phi)^{2.5}[1-\phi+\phi(\rho_s/\rho_f)]},$$

$$\Gamma_2(\phi) = \frac{1}{\left[1-\phi+\phi(\rho_s/\rho_f)\right]},$$

$$\Gamma_3(\phi) = \frac{\left[1-\phi+\phi\left((\rho\beta)_s/(\rho\beta)_f\right)\right]}{1-\phi+\phi(\rho_s/\rho_f)},$$

$$\Gamma_4(\phi) = \frac{1}{\left[1-\phi+\phi\left((\rho C_p)_s/(\rho C_p)_f\right)\right]} \tag{16}$$

Here Ha is the magnet parameter, $\delta_1$ and $\delta_2$ are the slip factors, respectively, where $\delta$ reflects to the slip ratio, Rd is the thermal radiation parameter, H is the surface temperature excess ratio, and Pr is the Prandtl number.

The local skin friction coefficients in the $x$- and $y$-orientations and local Nusselt number are an important parameters commonly used in fluid mechanics. The non-dimensional forms of these quantities are defined as [26]:

$$C_{fx} = \frac{2}{(1-\phi)^{2.5}\mathrm{Re}_x^{1/2}\sqrt{\tau}}\left(f''(\tau,0) + \frac{Gr_x}{\mathrm{Re}_x^2}\cos\Omega g'(\tau,0)\right), \tag{17}$$

$$C_{fy} = \frac{2Gr_x}{(1-\phi)^{2.5}\mathrm{Re}_x^{5/2}\sqrt{\tau}}\sin\Omega h'(\tau,0), \tag{18}$$

$$Nu_x = \frac{q_w x}{k_f(T_f - T_\infty)} = -\mathrm{Re}_x^{1/2}\tau^{-1/2}\left(\frac{k_{ff}}{k_f} + \frac{4H^3Rd}{3}\right)\theta'(\tau,0), \tag{19}$$

where $Gr_x = g^*\beta_f(T_f - T_\infty)x^3/{\upsilon_f}^2$ and $\mathrm{Re}_x = bx^2/\upsilon_f$ are the local Grashof and Reynolds number, respectively.

It is noteworthy to mention that by substituting $Rd = 0$, $\phi = 0$ and $\delta_1 = \delta_2 = 0$ in Eqs. (10)–(15), the problem is reduced to the transient MHD flow of regular fluid and heat transfer over an inclined stretching sheet which is discussed previously in [26].

## 3. Numerical method and validation

In the current study, Cobalt-kerosene ferrofluid with the impacts of anisotropic slip and thermal radiation is considered. The results were performed for the solid volume fraction $0.01 \le \phi \le 0.2$ [29], slip factor $0.1 \le \delta_1 \le 2.0$ [30], and to supply sufficient information, two various values of the magnet and thermal radiation parameters (Ha = 0.0, 2.0, Rd = 0.0, 5.0) have been considered [24].

The collection of nonlinear coupled Eqs. (10)–(14) are solved by the Thomas algorithm with finite difference technique to obtain the velocity, pressure and temperature distributions [31].The computational domain $0 \le \eta \le 35$, $0 \le \tau \le 5$ is divided into nodes with step sizes $\Delta\eta_1 = 0.001$ and $\Delta\tau_1 = 0.01$ for boundary layer and time, respectively. Convergence of the scheme is assumed when anyone of quantities $f$, $g$, $h$, $G$ and $\theta$ their gradients for last two approximations differ from unity by less than $10^{-6}$ for all values of $\eta$ and $\tau$. Computations are repeated until both the boundary layer and the dimensionless time are reached to the ambient conditions and maximum value, respectively. In order to validates the reliability of the current results with the results of [26] in Fig. 2 for various values of Pr and Ha at Rd = 0, $\phi = 0$, $\delta_1 = 0$ and $\delta_2 = 0$. As it is found from this Fig. a good agreement with those solutions.

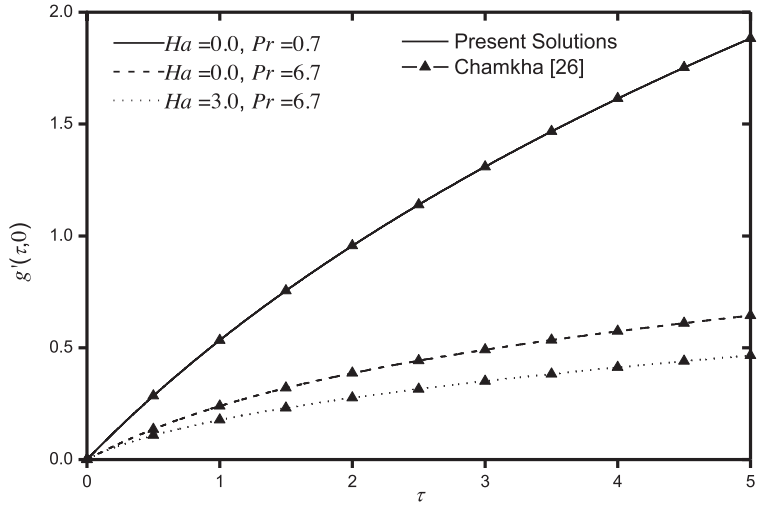


**Fig. 2.** Comparison between current solutions and Chamkha [26].

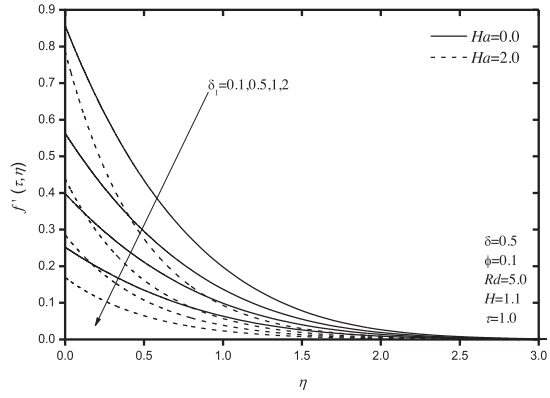


**Fig. 3.** Impact of $\delta_1$ on the velocity of $x$-orientation ($f'$).

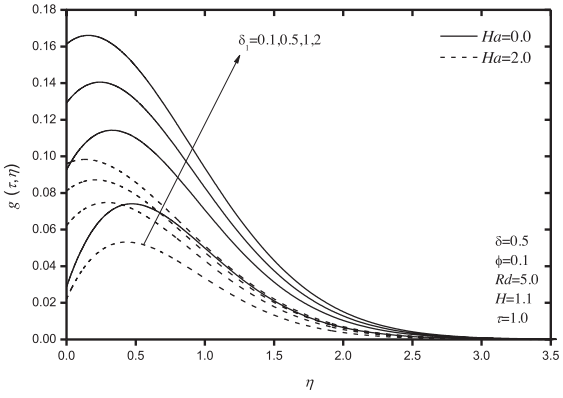


**Fig. 4.** Impacts of $\delta_1$ and Ha on the velocity of $x$- orientation ($g$).

Furthermore, a detailed description of the existence of multiple solutions is given by Turkyilmazoglu [32]. However, various attempts of this problem did not yield to the existence of multiple physical solutions.

## 4. Results and discussion

To obtain perspective of the flow regime, the impacts of various controlling parameters on velocity, temperature and pressure distributions are accomplished through graphs and also the physical nature is discussed in detail.

Figs. 3–11 reveal the impact of the magnet parameter Ha and the slip factor $\delta_1$ on the profiles of the ferrofluid velocity components in $x$- and y-orientations ($f'(\tau,\ \eta)$,$g(\tau,\ \eta)$), $h(\tau,\ \eta)$, pressure $G(\tau,\ \eta)$, and temperature $\theta(\tau,\ \eta)$, likewise the local skin-friction coefficients in the $x$- and $y$-orientations $C_{fx}$ and $C_{fy}$ and local Nusselt number $Nu_x$, respectively. It is noteworthy to mention from Figs. 2–5 that strengthening the magnet parameter is acted in the $y$-orientation which in turn induces the current in conductive fluid and creates a resistive-type force (Lorentz force) on the ferrofluid which retards the motion in both the $x$- and z-trends. Thus, an increase in Ha instigates a decrease in the $x$-velocity components ($f'$and $g$), and increase in $y$-velocity component $h$. As a consequence, both of temperature and pressure distributions have a predisposition to decrease due to the increment in the magnetic field as shown in Figs. 6 and 7. These graphs show also a considerable effect of this parameter on the hydrodynamic boundary-layer

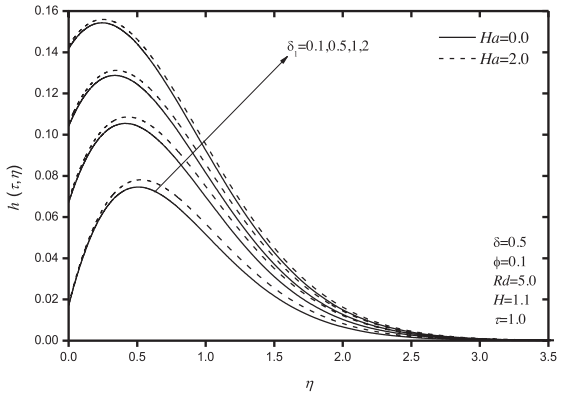


**Fig. 5.** Impacts of $\delta_1$ and Ha on the velocity of $y$- orientation ($h$).

thickness of the ferrofluid, i.e., this thickness decreases with the increase of *Ha*. Also, according to the definition of slip ratio $\delta$ in Eq. (7), it is apparent that the elevate in the slip factors $\delta_1$ and $\delta_2$ results in a considerable damp in both the $x$-velocity component $f'$and pressure distributions $G$, whereas the trend is reversed for the velocity of $x$-tendency $g$, velocity in $y$-tendency $h$, and ferrofluid temperature $\theta$. This is because the boost in the values of the velocity slip parameters $\delta_1$ and $\delta_2$ has a predilection to accelerate the motion in the $y$-tendency which is oblique to the horizontal streak, whereas a reverse trend occurred along the stretched sur-

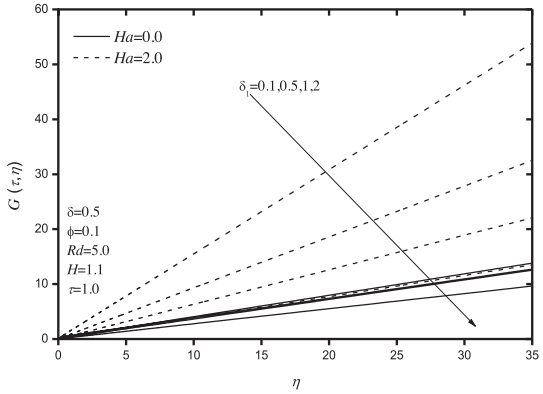


**Fig. 6.** Impacts of $\delta_1$ and Ha on the pressure profiles ($G$).

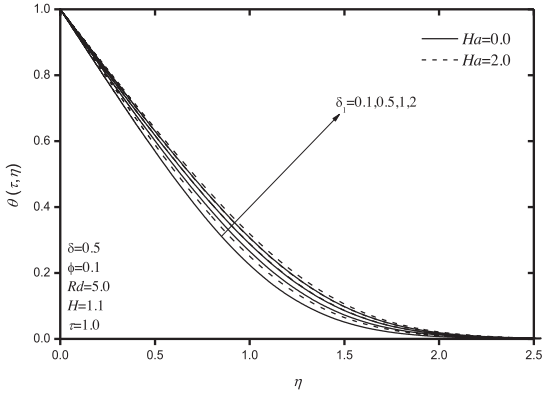


**Fig. 7.** Impacts of $\delta_1$ and Ha on the temperature ($\theta$).

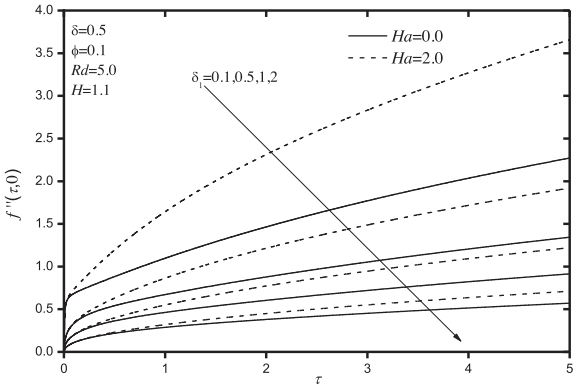


**Fig. 8.** Impacts of $\delta_1$ and Ha on the skin-friction coefficient in the $x$-orientation $f''(\tau, 0)$.

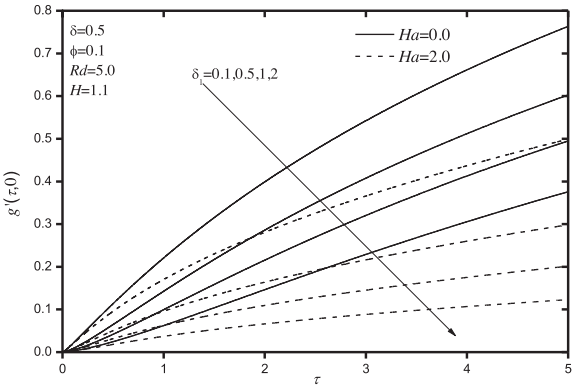


**Fig. 9.** Impacts of $\delta_1$ and Ha on the skin-friction coefficient in the $x$-orientation $g'(\tau, 0)$.

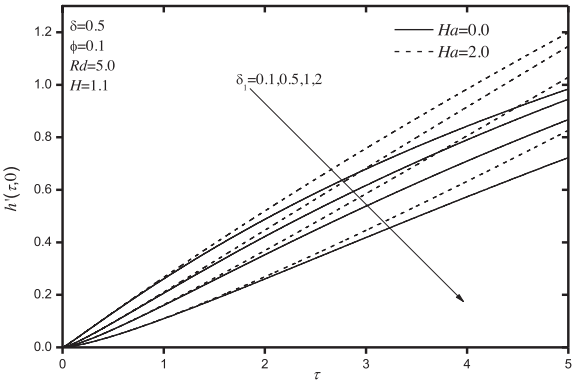


**Fig. 10.** Impacts of $\delta_1$ and Ha on the skin-friction coefficient in the $y$- orientation $h'(\tau, 0)$.

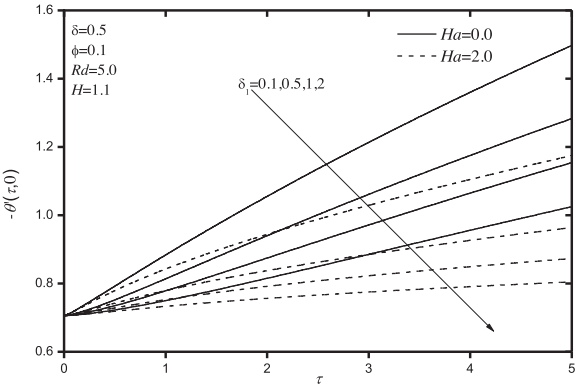


**Fig. 11.** Impacts of $\delta_1$ and Ha on the heat transfer$-\theta'(\tau, 0)$.

face in $x$-tendency. Physically this can be clarified as follows. When slip happens, the flow velocity near the sheet is no longer equal to the stretching velocity at the sheet. With the augmentation in $\delta_1$ and $\delta_2$, such slip velocity rises and then the ferrofluid velocity diminishes because under the slip condition at the boundary, the dragging of the stretching sheet can only partly be transmitted to the ferrofluid.

In addition, as seen from the definitions of $C_{fx}$, $C_{fy}$ and $Nu_x$, in Eqs. (17)–(19) they are immediately commensurate to$f''(\tau, 0)$,$g'(\tau, 0)$,$h'(\tau, 0)$and$-\theta'(\tau, 0)$, respectively. It is apparent from Figs. 8–11 that there are two adverse behaviors for the skin-friction coefficients and Nusselt number. These behaviors are clarified by an enhancement in the skin-friction coefficients in the $x$- and $y$-or $f''(\tau, 0)$, $h'(\tau, 0)$and a diminished in both the skin-friction coefficient in the $x$- orientation $g'(\tau, 0)$and Nusselt number$-\theta'(\tau, 0)$ occurred as the magnet parameter Ha boosts. This is due to the fact that the damp in the flow velocities close to the dike with an accretion in the ferrofluid temperature as Ha boosts, creating the magnitude of heat transfer to decrease. These results agree with the physical view as on applying the magnetic field to nanofluid, this gives a boost of the Lorentz force, which slows down the fluid movement. However, all the skin-friction coefficients and the magnitude of heat transfer are reduced as the slip factors elevated.

Figs 12–20 demonstrate the impacts of thermal radiation parameter Rd and solid volume fraction of ferrofluid $\phi$ upon variation velocity components, pressure, temperature behaviour along with local skin-friction coefficients and Nusselt number, respectively. From Fig. 12–16, it is manifested that an increment in the

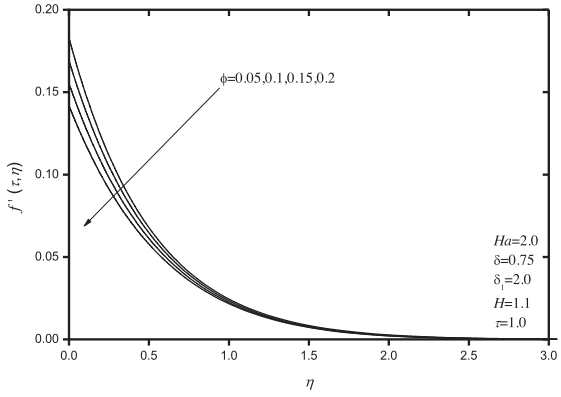


**Fig. 12.** Impacts of $\phi$ and Rd on the velocity of $x$-orientation ($f'$).

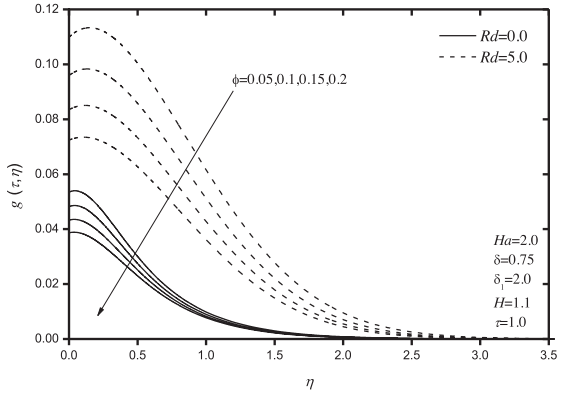


**Fig. 13.** Impacts of $\phi$ and Rd on the velocity of $x$-orientation ($g$).

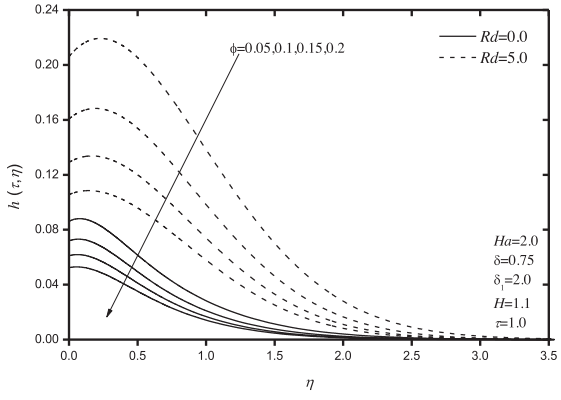


**Fig. 14.** Impacts of $\phi$ and Rd on the velocity of $y$-orientation ($h$).

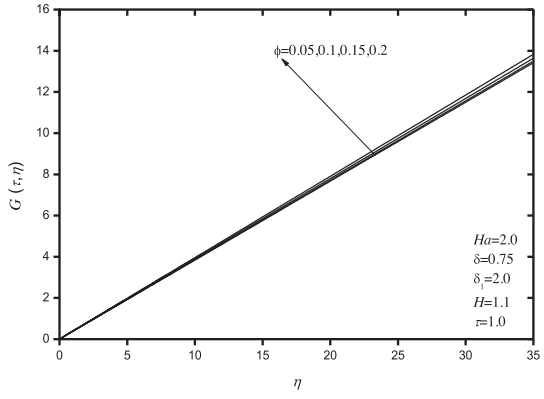


**Fig. 15.** Impacts of $\phi$ and Rd on the pressure profiles ($G$).

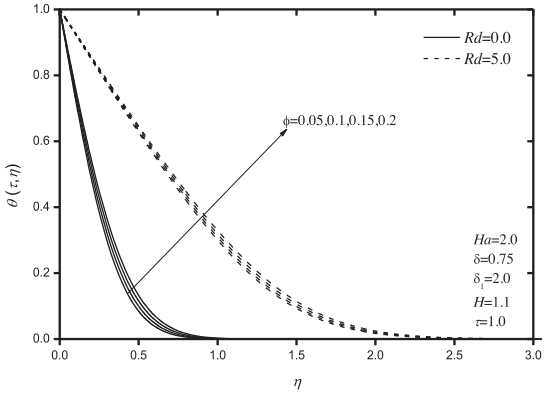


**Fig. 16.** Impacts of $\phi$ and Rd on the temperature ($\theta$).

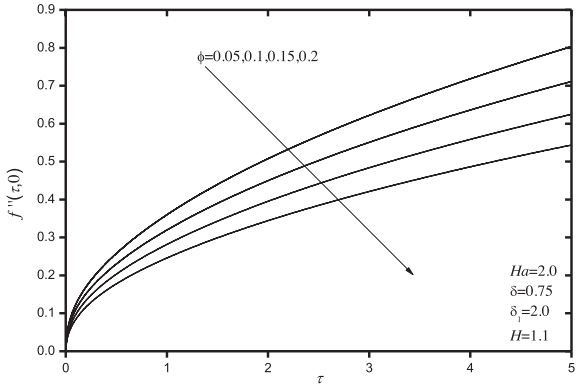


**Fig. 17.** Impact of $\phi$ on the skin-friction coefficient in the $x$-orientation $f''(\tau, 0)$.

solid volume fraction $\phi$ tends to damp the velocity components and to promote the distributions of pressure and ferrofluid temperature because higher values of $\phi$ correspond to booster thermal conductivity of ferrofluid (see Table 1) which stimulates the heat diffusion so that the heat precipitately diffuse near the stretched surface. this result of is match with the physical conduct because the increment in $\phi$ enhances the thermal conductivity of the base fluid and this leads to enhance the thermal diffusion in the boundary layer. On other side, an elevation in the radiation parameter Rd results in a considerable enhance in the velocity components in $x$- and $y$-orientations ($g$,$h$), and temperature distribution. The reason for this pattern is that, the presence of thermal radiation yields an enormous increase in the radiative heat which promotes the thermal state of the ferrofluid creating its temperature to enhance. As a result, this leads to a sufficient enhancement in the hydrodynamics and thermal boundary layer thickness. From Figs. 17–20, it is depicted that $f''(\tau, 0)$,$g'(\tau, 0)$,$h'(\tau, 0)$and$-\theta'(\tau, 0)$are diminished for amplifying $\phi$ because an increase in $\phi$ reduces the shear stress and heat transfer by increasing the ferrofluid viscosity. Actuality, utilizing smaller nanoparticles achieves a better thermal performance. However, in the evaluation of the effects various nanofluids, Turkyilmazoglu [33] proposed an interesting rescaling approach that greatly simplifies the evaluation of flow and physical parameters such as skin friction and heat transfer rate based on the solution of the single phase flow without the nanoparticles.

Moreover, it is noteworthy to mention that based on Eq. (19), the increment in the thermal radiation has a tendency to enhance the skin friction coefficients and Nusselt number. This corresponds with the physical trend that, as apparent from Eq. (19), the heat transfer becomes greater in the existence of the radiation impact, and hence the shear stress evolves. Also, the impact of solid vol-

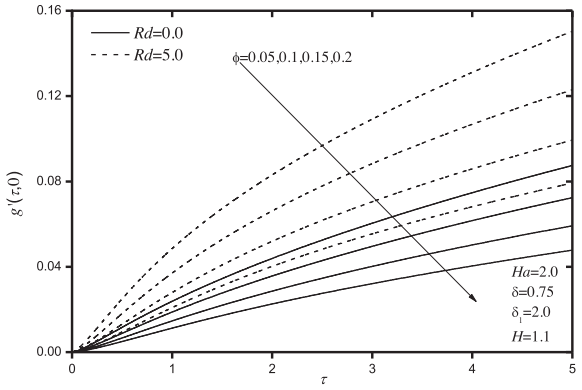


**Fig. 18.** Impacts of $\phi$ and Rd on the skin-friction coefficient in the $x$-orientation $g'(\tau, 0)$.

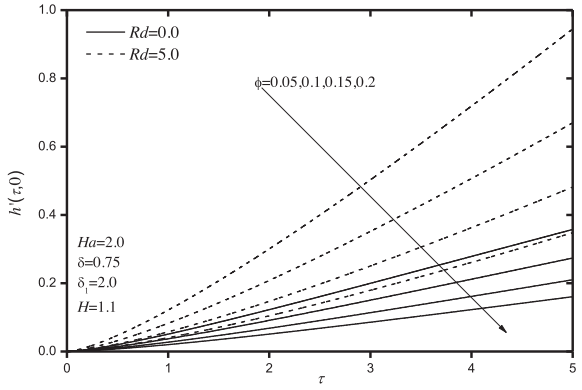


**Fig. 19.** Impacts of $\phi$ and Rd on the skin-friction coefficient in the $y$-orientation $h'(\tau, 0)$.

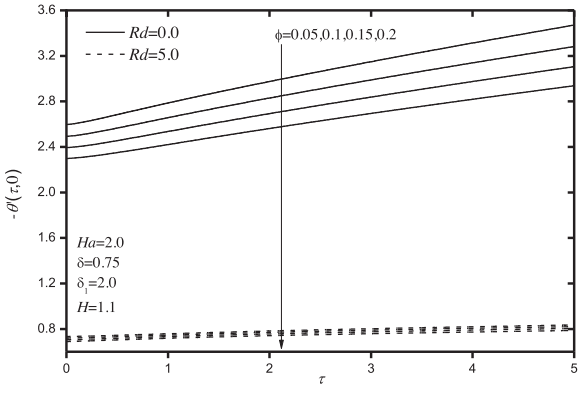


**Fig. 20.** Impacts of $\phi$ and Rd on the heat transfer $-\theta'(\tau, 0)$.

ume fraction for heat transfer is more prevalent the existence of thermal radiation than its absence. The reason for this behavior is that, the existence of thermal radiation implies a huge enhancement in the radiative heat which elevates the thermal state of the ferrofluid causing its temperature to enhance.

## 5. Conclusions

This investigation is ensued to examine the impact of anisotropic slip on transient three dimensional MHD flow of ferrofluid over a radiate stretching surface. The governing equations are solved by implicit numerical scheme of finite-difference type and the impacts of various significant parameters on flow and heat transfer are accomplished through graphs. The present investigation brings out the following outcomes:

1. The fluid velocity components are accelerated for increasing the slip factors and thermal radiation parameter whereas the trend is reversed for the solid volume fraction and magnet parameters.
2. The heat transfer elevates with boosting values of radiation parameter while diminishes for higher values of solid volume fraction, magnet parameter and slip factors.
3. Increasing the solid volume fraction and slip factors inhibit the skin-friction coefficients whereas the behavior is reversed for the magnet and radiation parameters.

## Acknowledgment

Author thank Anonymous reviewers for critical comments and suggestions which improved the quality of the manuscript.

## References

[1] S.I. Pai, Magnetogasdynamics and Plasma Dynamics, Springer, Berlin, 1962.
[2] I. Liuta, F. Larachi, Magnetohydrodynamics of trickle bed reactors: mechanistic model, experimental validation and simulations, Chem Eng Sci 58 (2003) 297–307.
[3] T. Hayat, A. Shafiq, A. Alsaedi, M. Awais, MHD axisymmetric flow of third grade fluid between stretching sheets with heat transfer, Comput. Fluids 86 (2013) 103–108.
[4] A.A. Afify, M.J. Uddin, M. Ferdows, Scaling group transformation for MHD boundary layer flow over permeable stretching sheet in presence of slip flow with Newtonian heating effects, Appl. Math. Mech. -Engl. Ed. 35 (11) (2014) 1375–1386.
[5] T. Hayat, A. Shafiq, A. Alsaedi, S.A. Shahzad, Unsteady MHD flow over exponentially stretching sheet with slip conditions, Appl. Math. Mech. -Engl. Ed. 37 (2) (2016) 193–208.
[6] S.K. Das, S.U.S. Choi, W. Yu, T. Pradeep, Nanofluids-Science and Technology, John Wiley & Sons Publishers, Hoboken, 2007.
[7] J. Buongiorno, Convective transport in nanofluids, ASME J. Heat Transfer 128 (2006) 240–250.
[8] R.K. Tiwari, M.K. Das, Heat transfer augmentation in a two-sided lid-driven differentially heated square cavity utilizing nanofluids, *Int. J Heat Mass Tran*fer 50 (2007) 2002–2018.
[9] F.M. Hady, F.S. Ibrahim, S.M. Abdel-Gaied, Radiation effect on viscous flow of a nanofluid and heat transfer over a nonlinearly stretching sheet, Nanoscale. Res. Lett. 7 (2012) 229–236.
[10] A.J. Chamkha, S. Abbasbandy, A.M. Rashad, K. Vajravelu, Radiation effects on mixed convection over a wedge embedded in a porous medium filled with a nanofluid, Transp. Porous Medium 91 (2012) 261–279.
[11] A.J. Chamkha, S. Abbasbandy, A.M. Rashad, K. Vajravelu, Radiation effects on mixed convection about a cone embedded in a porous medium filled with a nanofluid, Meccanica 48 (2013) 275–285.
[12] O.A. Bég, M. Ferdows, Explicit numerical simulation of magnetohydrodynamic nanofluid flow from an exponential stretching sheet in porous media, Appl. Nanosci. (2013) 1–15, doi:10.1007/s13204-013-0275-0.
[13] S.M.M. EL-Kabeir, Ali.J. Chamkha, A.M. Rashad, The effect of thermal radiation on non-Darcy free convection from a vertical cylinder embedded in a nanofluid porous media, J. Porous Media 17 (3) (2014) 269–278.
[14] J. Zhu, L. Zheng, L. Zheng, X. Zhang, Second-order slip MHD flow and heat transfer of nanofluids with thermal radiation and chemical reaction, Appl. Math. Mech. -Engl. Ed. 36 (9) (2015) 1131–1146.
[15] S.M.M. EL-Kabeir, M. Modather, A.M. Rashad, Effect of thermal radiation on mixed convection flow of a nanofluid about a solid sphere in a saturated porous medium under convective boundary condition, J. Porous Media 18 (6) (2015) 569–584.
[16] M. Turkyilmazoglu, Analytical solutions of single and multi-phase models for the condensation of nanofluid film flow and heat transfer, Eur. J. Mech. B. Fluids 53 (2015) 272–277.
[17] B.M. Berkovsky, V.F. Medvdev, M.S. Krakov, Magnetic Fluids, Engineering Applications, Oxford University Press, Oxford, 1973.
[18] R.E. Rosensweig, Ferrohydrodynamics, Cambridge University Press, London, 1985.
[19] M.S. Kandelousi, R. Ellahi, Simulation of ferrofluid flow for magnetic drug targeting, Z. Naturforsch (2015) 1–10.
[20] A. Zeeshan, R. Ellahi, M. Hassan, Magnetohydrodynamic flow of water/ethylene glycol based nanofluids with natural convection through a porous medium, Eur. Phys. J. Plus 129 (2014) 261.
[21] A. Malvandi, A. Ghasemi, D.D. Ganji, Thermal performance analysis of hydromagnetic $Al_2O_3$-water nanofluid flows inside a concentric microannulus considering nanoparticle migration and asymmetric heating, Int. J. Therm. Sci. 109 (2016) 10–22.

[22] S. Heysiattalab, A. Malvandi, D.D. Ganji, Anisotropic behavior of magnetic nanofluids (MNFs) at filmwise condensation over a vertical plate in presence of a uniform variable directional magnetic field, J. Mol. Liq. 219 (2016) 875–882.
[23] A. Malvandi, S. Heysiattalab, D.D. Ganji, Effects of magnetic field strength and direction on anisotropic thermal conductivity of ferrofluids (magnetic nanofluids) at filmwise condensation over a vertical cylinder, Adv. Powder Technol. 27 (4) (2016) 1539–1546.
[24] A.M. Rashad, Impact of thermal radiation on MHD slip flow of a ferrofluid over a non-isothermal wedge, J. Magn. Magn. Mater. 422 (2017) 25–31.
[25] M. Sheikholeslami, M. Gorji-Bandpy, Free convection of ferrofluid in a cavity heated from below in the presence of an external magnetic field, Power Technol. 256 (2014) 490–498.
[26] A.J. Chamkha, Transient hydromagnetic three-dimensional natural convection from an inclined stretching permeable surface, Chem. Eng. J. 76 (2000) 159–168.
[27] J. Maxwell, A Treatise on Electricity and Magnetism, second ed., Oxford University Press, Cambridge, UK, 1904.
[28] R. Siegel, J.R. Howell, Thermal Radiation Heat Transfer, McGraw-Hill, New York, 1972.
[29] M. Turkyilmazoglu, Nanofluid flow and heat transfer due to a rotating disk, Comput. Fluids 94 (2014) 139–146.
[30] A. Raees, M. Ul-Haq, H. Xu, Q. Sun, Three-dimensional stagnation flow of a nanofluid containing both nanoparticles and microorganisms on a moving surface with anisotropic slip, Appl. Math. Modell. 40 (5-6) (2016) 4136–4150.
[31] F.G. Blottner, Finite-difference methods of solution of the boundary-layer equations, AIAA J. 8 (1970) 193–205.
[32] M. Turkyilmazoglu, Exact multiple solutions for the slip flow and heat transfer in a converging channel, J. Heat Transfer 137 (2015) 101301–1013018.
[33] M. Turkyilmazoglu, A note on the correspondence between certain nanofluid flows and standard fluid flows, J. Heat Transfer 137 (2015) 024501.